EARTHQUAKE ENGINEERING AND STRUCTURAL DYNAMICS
Earthquake Engng Struct. Dyn. 2007; **36**:927–948
Published online 28 November 2006 in Wiley InterScience (www.interscience.wiley.com). DOI: 10.1002/eqe.662

Effect of near-fault ground motion and damper characteristics on the seismic performance of chevron braced steel frames

Murat Dicleli[1,*,†,‡] and Anshu Mehta[2,§]

[1]*Department of Engineering Sciences, Middle East Technical University, Ankara 06531, Turkey*
[2]*Department of Civil Engineering and Construction, Bradley University, Peoria, IL 61625, U.S.A.*

SUMMARY

This study is aimed at comparing the seismic performance of steel chevron braced frames (CBFs) with and without fluid viscous dampers (FVDs) as a function of the characteristics of the near-fault (NF) ground motion and FVD parameters. For this purpose, comparative nonlinear time history (NLTH) analyses of single and multiple storey CBFs with and without FVDs are conducted using NF ground motions with various velocity pulse periods scaled to have small, moderate and large intensities. Additionally, NLTH analyses of single- and four-storey CBFs with FVDs are conducted to study the effect of the damping ratio and velocity exponent of the FVD on the seismic performance of the frames. The analyses results revealed that the seismic performance of the CBFs without FVDs is very poor and sensitive to the velocity pulse period and the intensity of the NF ground motion due to brace-buckling effects. Installing FVDs into the CBFs significantly improved their seismic performance by maintaining their elastic behaviour. Furthermore, FVDs with smaller velocity exponents and larger damping ratio are observed to be more effective in improving the seismic performance of the CBFs subjected to NF earthquakes. However, FVDs with damping ratios larger than 50% do not produce significant additional improvement in the seismic performance of the CBFs. Copyright © 2006 John Wiley & Sons, Ltd.

Received 28 June 2006; Revised 27 October 2006; Accepted 27 October 2006

KEY WORDS: steel; frame; bracing; damper; seismic; near fault

INTRODUCTION

In steel building construction, chevron braced frame (CBF) is frequently used since its brace configuration provides an open space for architectural arrangements. Seismic energy dissipation in a CBF solely depends on the inelastic cyclic behaviour of the braces. Cyclic axial force–deformation behaviour of a brace is unsymmetric in tension and compression and typically exhibits substantial strength and stiffness deterioration due to buckling effects [1]. Thus, when subjected to a strong

*Correspondence to: Murat Dicleli, Department of Engineering Sciences, Middle East Technical University, Ankara 06531, Turkey.
†E-mail: mdicleli@metu.edu.tr
‡Associate Professor.
§Graduate Research Assistant.

ground motion, inelastic buckling of the braces in a CBF results in loss of lateral stiffness and strength of the frame [2]. Furthermore, it is difficult to achieve well-distributed ductility demands along the height of the CBF due to the premature buckling of the braces at certain floor levels [3], which results in soft-storey formations, dynamic instability [4] and hence substantial damage to the frame members. Because of the above-mentioned poor performance characteristics, a large number of CBFs suffered considerable damage in past earthquakes [5–10].

Near-fault (NF) ground motions affected by directivity contain distinct pulses in their acceleration and velocity histories. For the same peak ground acceleration (A_p) and duration of shaking, NF ground motions with forward rupture directivity effect can generate much higher base shears and inter-storey drifts in buildings compared to those produced by far-fault ground motions [11]. Thus, such ground motions are anticipated to be even more detrimental to CBFs, which have already been observed to suffer substantial damage in past earthquakes.

Numerous research studies have been initiated in recent years to improve the performance of CBFs through the introduction of new structural configurations [2, 12], the use of high-performance materials [13], buckling restrained braces [1] as well as passive energy dissipation devices such as hysteretic [14], friction [15] and fluid viscous dampers (FVDs) [16–18]. Among all these seismic performance improvement techniques, using FVDs in a structure has the unique advantage of reducing the structure base shear force and deflections at the same time since the velocity-dependent maximum FVD force is out of phase with the maximum deflection of the structure [18]. In addition, installing FVDs into a structure does not alter its force–displacement relationship and hence its dynamic modal characteristics [19]. Furthermore, since NF ground motions with forward rupture directivity effect are generally composed of one or more, high-amplitude, long-period velocity pulses, it is anticipated that, when installed in CBFs, the velocity-dependent FVDs may mitigate the effect of such high-velocity jolts efficiently. Consequently, FVDs seem to be viable tools for improving the seismic performance of CBFs located within NF zones.

Many research studies concerning the effect of FVDs on the seismic performance of building structures subjected to far-fault [17–21] and NF [22–25] ground motions have been conducted in the past. However, a comparative research study on the seismic performance of CBFs with and without FVDs as a function of NF ground motion and damper parameters is scarce. Furthermore, it is important to evaluate the efficiency and feasibility of nonlinear FVDs, which are particularly used to obtain smaller damper forces in retrofitting applications, for mitigating the detrimental effects of NF ground motions. It is also important to evaluate the efficiency and feasibility of using FVDs with higher damping constants to mitigate the effects of intense velocity pulses associated with NF ground motions. Thus, this study focuses on comparing the seismic performance of CBFs with and without FVDs as a function of the intensity and frequency characteristics of the NF ground motion as well as the damping ratio and velocity exponent of the FVD. The results from such a research study may then be used to measure the efficiency of FVDs for improving the seismic performance of CBFs as a function of the NF ground motion characteristics and FVD parameters and arrive at important conclusions and recommendations related to the seismic retrofitting and design of CBFs located near active faults using FVDs.

RESEARCH OUTLINE

In this research, first, a numerical brace-buckling model is developed to simulate the inelastic cyclic behaviour of the braces in CBFs using the finite-element-based program ADINA [26]. Next,

DOI: 10.1002/eqe

84 comparative nonlinear time history (NLTH) analyses of single, two, four and eight-storey CBFs with and without FVDs are conducted using seven NF ground motions with various velocity pulse periods scaled to represent small, moderate and large intensity earthquakes. These comparative analyses are performed mainly to study the effect of the NF ground motion properties and the number of stories on the seismic performance of CBFs with and without FVDs. Subsequently, 224 additional NLTH analyses of single and four-storey CBFs with FVDs are conducted to study the effect of the damping ratio and velocity exponent of the FVD on the seismic performance of the frames as a function of the NF ground motion parameters. In the last phase of the research, practical implications of using FVDs in CBFs are outlined and important conclusions and recommendations collected from the NLTH analyses results are summarized.

DETAILS OF THE FRAMES CONSIDERED FOR ANALYSES

The details of the one, two, four and eight-storey frames considered for NLTH analyses are demonstrated in Figure 1. The frame members are numbered from 1 to 11 and their sizes are tabulated across each number in the same figure. First, the eight-storey frame is configured such that each two-storey levels have the same member sizes, the lateral strength of the frame gradually decreases at the higher storey levels and the frame exhibits nonlinear behaviour under moderate to high intensity ground motions per current state of practice. The one, two and four-storey frames are

Member No	Member size
1	W310x158
2	W310x129
3	HSS127x127x6
4	W310x118
5	W310x97
6	W310x52
7	W310x45
8	HSS102x102x8
9	W250x45
10	W250x39
11	HSS89x89x6

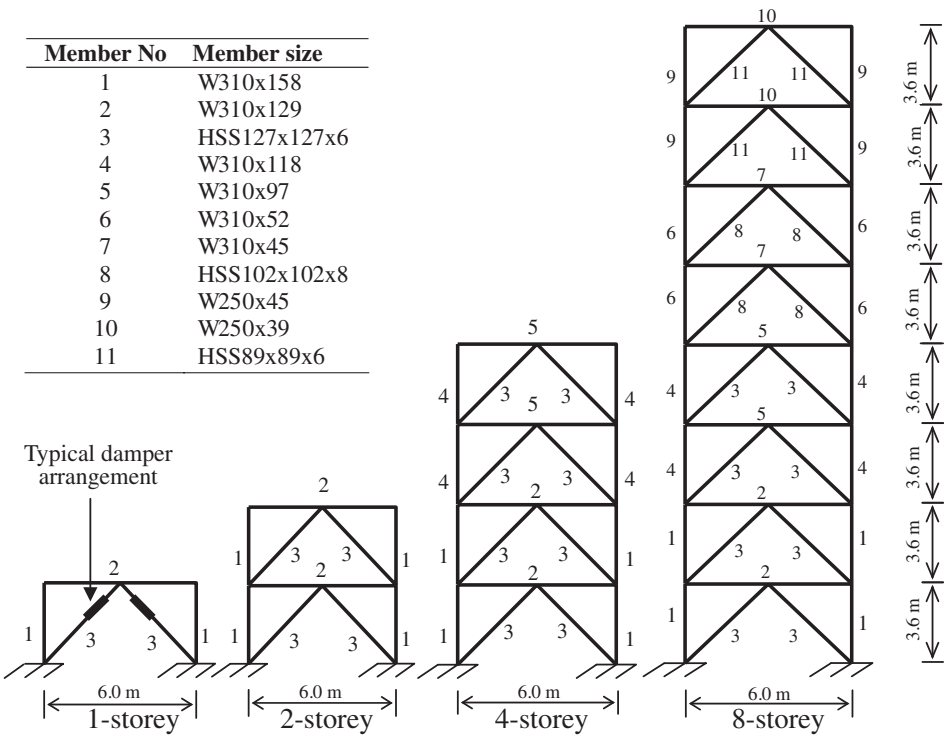

Figure 1. Frame models.

DOI: 10.1002/eqe

Table I. Properties of near-fault ground motions used in the analyses.

Earthquake	Station	Distance (km)	A_p (g)	V_p (cm/s)	T_p (s)
Morgan Hill, 1984	Gilroy 6	11.8	0.29	36.4	1.10
Northridge, 1994	Rinaldi	7.1	0.84	166.1	1.25
Loma Prieta, 1989	Gilroy 2090	12.7	0.34	39.1	1.40
Northridge, 1994	Sylmar Olive view	6.1	0.35	116.3	2.60
Imperial Valley, 1940	Impvall/H-ECC092	7.6	0.37	69.0	3.30
Imperial Valley, 1940	Impvall/H-E05230	1.0	0.24	90.5	3.90
Landers, 1992	Lucerne	1.1	0.72	97.6	5.00

then assumed to form the bottom one, two and four stories of the eight-storey frame, respectively. This was done solely to study the performance of the CBFs with and without FVDs as a function of the number of stories. The fundamental periods of the one, two, four and eight-storey CBFs are 0.23, 0.28, 0.39 and 0.67 s, respectively. For the CBFs with FVDs, the dampers are assumed to be mounted along the existing chevron braces. A typical FVD arrangement is illustrated on the single-storey frame in Figure 1.

GROUND MOTIONS CONSIDERED FOR ANALYSES

NF ground motions are generally characterized by their peak ground velocity, V_p (or acceleration, A_p) and velocity pulse period, T_p, representing their dominant period and energy content. Consequently, NF ground motions with various velocity pulse periods and intensities are considered to assess the performance of the CBFs with and without FVDs for a wide range of NF ground motion characteristics. For this purpose, a set of seven NF ground motions with velocity pulse periods ranging between 1.1 and 5.0 s are considered (Table I). Recent research [27] on measuring the intensity of NF ground motions revealed that the peak ground acceleration is a better representative intensity measure than the peak ground velocity. Accordingly, the peak accelerations of the NF ground motions are scaled to have $A_p = 0.20$, 0.35 and $0.50g$ representing, respectively, small, moderate and large intensity earthquakes.

BRIEF REVIEW OF FLUID VISCOUS DAMPERS

FVDs operate on the principle of fluid flow through orifices. Details of a typical FVD are illustrated in Figure 2(a). An FVD consists of a piston within a damper housing filled with a compound of compressible silicone fluid. The piston head contains a number of small orifices through which the fluid passes from one side of the piston to the other. Thus, the FVD dissipates the earthquake input energy through the movement of a piston in a highly viscous fluid based on the concept of fluid orificing [28]. The force, F, in an FVD is calculated as

$$F = C\,\mathrm{sgn}(V)V^{\alpha} \tag{1}$$

where C is the damping constant, V is the velocity at which the damper is oscillating and α is the velocity exponent. A pure FVD force *versus* displacement hysteresis loop under a constant amplitude harmonic excitation is presented in Figure 2(b). The simplest form of FVD is a linear FVD, for which the velocity exponent, α, is equal to 1.0. Typical values of α range between 0.5

DOI: 10.1002/eqe

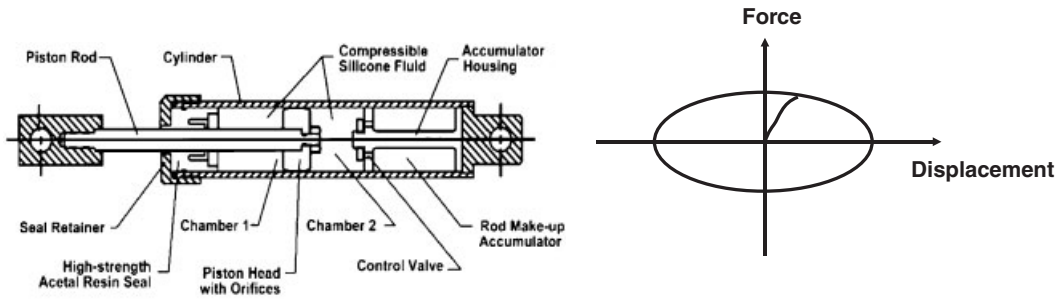

Figure 2. (a) Typical detail of a fluid viscous damper (Taylor Devices Inc.); and (b) force–displacement loop of a fluid viscous damper.

and 2.0 [29]. FVDs with α larger than 1.0 are generally not used in seismic design applications. Those with α smaller than 1.0 are called nonlinear FVDs.

For a multiple storey CBF with FVDs mounted diagonally along the chevron braces, the damping ratio, ζ_k, of the frame at the kth mode of vibration is expressed as [16]

$$\xi_k = \frac{\sum_j C_j \cos^2\theta(\phi_j - \phi_{j-1})^2}{2\omega_k \sum_j m_j \phi_j^2} \tag{2}$$

where C_j is the sum of the damping constants of the FVDs at the jth storey level, θ is the angle of inclination of the FVDs at the jth storey level, Φ_j is the modal displacement of the jth floor in the kth mode of vibration, ω_k is the unretrofitted circular frequency in the kth mode of vibration and m_j is the mass of the jth floor. In seismic design applications, typical damping ratios in the first mode of vibration range between 10 and 50%.

MODELLING OF THE CBF FOR NLTH ANALYSES

A direct integration NLTH analysis procedure is adopted to perform the seismic analyses of the frames using the nonlinear finite-element-based program ADINA. An implicit time integration procedure employing Newmark's method with $\delta = \frac{1}{2}$ and $\alpha = \frac{1}{4}$ was used in the solution. A 5% mass proportional Rayleigh structural damping [30] is used in the analyses of the frames. To calculate the structural damping constant, the Rayleigh mass proportionality factors for each frame are obtained based on the natural circular frequencies of their first vibration mode, which are obtained from eigenvalue analyses of the frames.

Modelling of brace inelastic cyclic behaviour in CBFs without FVDs

In a CBF, principally the inelastic cyclic behaviour of the braces results in the dissipation of earthquake energy. Hence, an accurate numerical simulation of this behaviour including buckling effects is required in the analyses.

The inelastic behaviour of steel braces is generally expressed in terms of an axial load, P, an axial displacement, δ, and a transverse displacement, Δ, at the mid-point of the brace as shown in

DOI: 10.1002/eqe

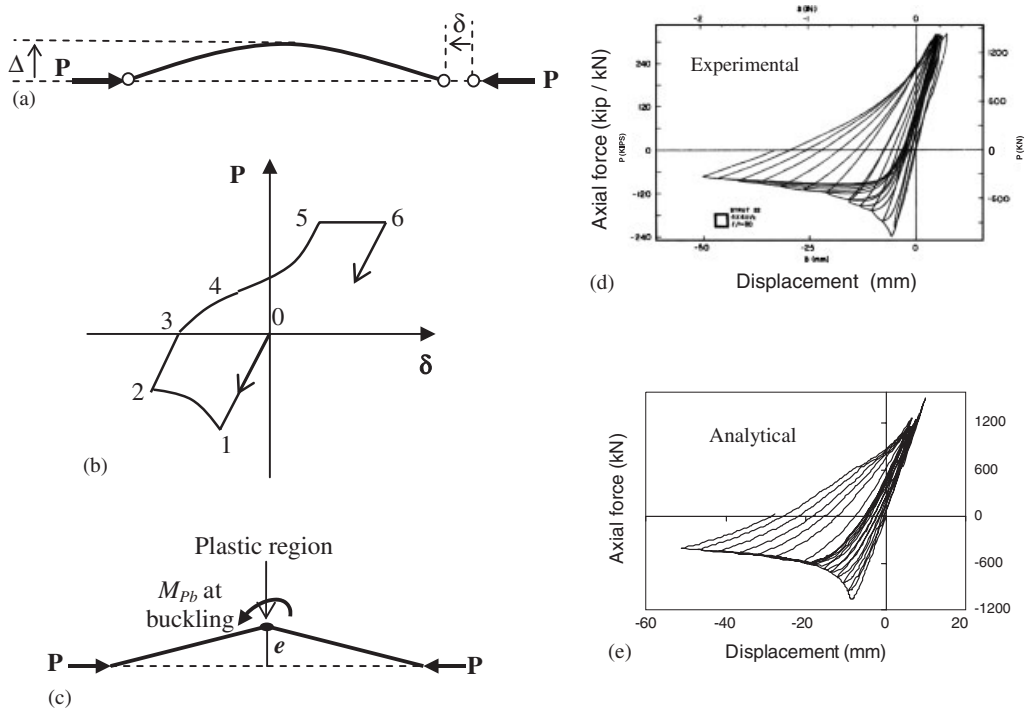

Figure 3. (a) Buckling brace; (b) typical brace axial force–deformation behaviour; (c) nonlinear brace model; (d) experimental hysteresis loop [31]; and (e) numerical hysteresis loop from ADINA.

Figure 3(a). A typical buckling curve of a brace member under cyclic axial load is illustrated in Figure 3(b) [32]. Starting from the unloaded condition, 0, in the figure, the brace is compressed in the linearly elastic range along segment 0–1. Due to the initial imperfections within the brace, second-order effects are generated under the applied axial load and the brace deflects transversely as demonstrated in Figure 3(a). Accordingly, in addition to the axial load, the brace is subjected to second-order moments along its length. The largest value of the second-order moment occurs at the mid-point of the brace ($P \times \Delta$) where the transverse displacement is maximum. At a critical value of the transverse displacement of the brace, the second-order moment in the brace will be equal to its plastic moment capacity under the applied axial load. At this point, the buckling load (point 1) is reached. Additional increases in the axial displacement result in larger transverse displacement, Δ, because of the plastic hinge rotations at the mid-point of the brace. Consequently, the second-order moment at the mid-point of the brace increases. This results in a drop in the axial force resistance of the brace along segment 1–2 due to the moment–axial force interaction effects. Upon unloading from point 2 to a level where the axial load is zero (point 3), the brace retains residual axial (δ) and transverse (Δ) deformations. When the brace is loaded in tension from point 3 to point 4, the behaviour is elastic. At point 4, the product of the axial load and transverse displacement again equals the plastic moment capacity of the brace under the applied axial load. Thus, a plastic hinge at the mid-point of the brace is produced for the second time. However, along segment 4–5, the plastic hinge rotations act in the reverse direction of that along

DOI: 10.1002/eqe

segment 1–2 and reduce the magnitude of the transverse deflection until the yield point (5) in tension is reached.

To simulate the inelastic cyclic behaviour described above, a numerical brace model shown in Figure 3(c) is developed in ADINA. An imperfection, e, is introduced at the centre of the brace to produce a kinked element for simulating the global buckling effects using large displacement analysis procedure. This initial imperfection is very small (generally 0.002–0.005 times the brace length) and does not alter the general axial force–deformation behaviour of the brace element. The imperfection, e, is given by the following equation [33]

$$e = \frac{M_{\mathrm{pb}}}{P_{\mathrm{b}}}\left(1 - \frac{P_{\mathrm{b}}L^2}{12EI}\right) \tag{3}$$

where L, E, I and M_{pb} are, respectively, the length, elastic modulus, moment of inertia and the reduced plastic moment capacity of the brace at buckling load. The imperfection is calculated such that when the axial load reaches the buckling load, the plastic moment capacity is reached at the vertex of the kinked brace element due to second-order effects. Beyond this point, the axial load capacity of the brace constantly decreases due to the combined effects of increasing second-order moments and moment–axial force interaction as the member buckles. Accordingly, a plastic hinge region accounting for moment–axial force interaction is defined at the vertex of the kinked brace element using a set of axial-force–moment–curvature relationships for the brace. Furthermore, the inelastic axial stress–strain relationship of the brace is defined to simulate its nonlinear behaviour in tension.

Figure 3(d) and (e) shows, respectively, the experimental [31] and numerical axial force–displacement hysteresis loops for a tubular brace member (TS4 $\times$ 4 $\times$ $\frac{1}{2}$) with a slenderness ratio of 80. The brace is subjected to gradually increasing cyclic axial displacements. From the comparison of the two figures it is clear that the general characteristics of the hysteresis loop of the numerical model are similar to those of the experimental model. Thus, it is used in the analyses of the CBF to model the nonlinear cyclic behaviour of the braces.

Modelling of CBF with nonlinear FVDs

The frames with FVDs are modelled in ADINA by adding damper elements to each of the braces. The damper element in ADINA requires the input of the damping constant C and the velocity exponent, α. For a specified value of damping ratio, ζ, at the first vibration mode of the frame, the value of the damping constant, C_j at each storey level j, is calculated from Equation (2) assuming that all the dampers within the frame have identical properties. The modal parameters in Equation (2) are obtained from the eigenvalue analyses of the frames. The calculated damping constant at each storey level is then divided by two and assigned to each damper element mounted along the two braces. The calculated damping ratios, ζ, are solely used as reference values in the figures throughout the paper to demonstrate the effect of increasing level of damping on the seismic response of the CBFs with FVDs, regardless of the α values considered in the analyses.

COMPARATIVE SEISMIC ANALYSES OF CBFs WITH AND WITHOUT FVDs

To study the effect of FVDs on the seismic performance of CBFs, a damping ratio of 50% of critical damping in the first mode of vibration is considered for the calculation of the damping constants of the FVDs in the structural model. Although a 50% damping ratio may be considered

DOI: 10.1002/eqe

large in some practical applications, it was chosen to clearly observe the difference between the seismic behaviour of CBFs with and without FVDs considering the high-velocity pulses of NF ground motions. Damping values smaller than 50% of critical (10 and 30%) are considered in the parametric studies presented in the subsequent sections. The dampers are assumed to be nonlinear with the velocity exponent, α, having a value of 0.5. A total of 84 NLTH analyses are conducted. The analyses results are discussed in the following subsections.

Performance of CBF with and without FVDs in relation to NF ground motion intensity

In this section, performances of the CBFs with and without FVDs are compared and studied in relation to the intensity of the NF ground motions. The analyses results are presented in Figures 4(a)–(c). Figure 4(a) compares the average of the maximum inter-storey drifts from the seven NF earthquakes for one, two, four and eight-storey CBFs with and without FVDs as a function of the intensity of the ground motions. For all the ground motion intensities and CBFs considered, the presence of FVDs produces significant improvements in the seismic response of the frames. The energy dissipated by the FVDs causes the frame members and the braces to remain within their elastic limits. It is noteworthy that the maximum damper forces shown in Figure 5(a) for four and eight-storey frames are smaller than the buckling capacity of the braces in the CBFs without FVDs. This results in considerably smaller inter-storey drifts of the CBFs with FVDs than those without FVDs. Furthermore, it is observed from Figure 4(b) that the ratios of the average maximum inter-storey drifts of the CBFs without FVDs to those with FVDs range between 1.65 and 9.85. In most structures equipped with FVDs, the reduction in the seismic drift response is in the order of 1.5–2.5 times. The larger reduction in the seismic drift response of CBFs (1.65–9.85) is partly due to (i) the buckling of the braces in CBFs without FVDs yielding unusually large inter-storey drifts compared to other types of structures and (ii) the relatively more efficient dissipation of the earthquake energy, which is transmitted by high-amplitude velocity pulses, by velocity-dependent FVDs. Thus, FVDs are observed to be very efficient devices for mitigating the effect of seismic forces particularly for CBFs located in NF zones. Moreover, it is observed from Figure 4(b) that the ratio of the average maximum drift of the CBF without FVD to that with FVD (drift ratio) is a function of the intensity of the NF ground motion and the number of stories. The dependency of this drift ratio on the intensity of the NF ground motion and the number of stories is found to result from the buckling of the braces. Buckling of the braces in CBFs without FVDs is generally more predominant for frames with larger number of stories subjected to NF ground motions with larger intensities. In such frames, the buckling of the braces at certain floor levels results in soft-storey formations. This, in turn, produces considerable plastic penetrations into the essential structural components of the CBFs that lead to large inter-storey drifts and hence large drift ratios.

In summary, it is found that using FVDs forms an effective design and retrofit strategy for CBFs and it is generally more useful for frames with larger number of stories located in NF zones with a high risk of intense earthquakes. Moreover, in retrofitting applications, the presence of the braces in CBFs is anticipated to facilitate the installation of the FVDs at relatively lesser cost compared to other types of structures such as moment-resisting frames.

Performance of the CBF with and without FVDs in relation to the velocity pulse period of the NF ground motion

In this section, performances of the CBFs with and without FVDs are compared and studied in relation to the velocity pulse period, T_p, of the NF ground motion. Figure 4(c) compares the

DOI: 10.1002/eqe

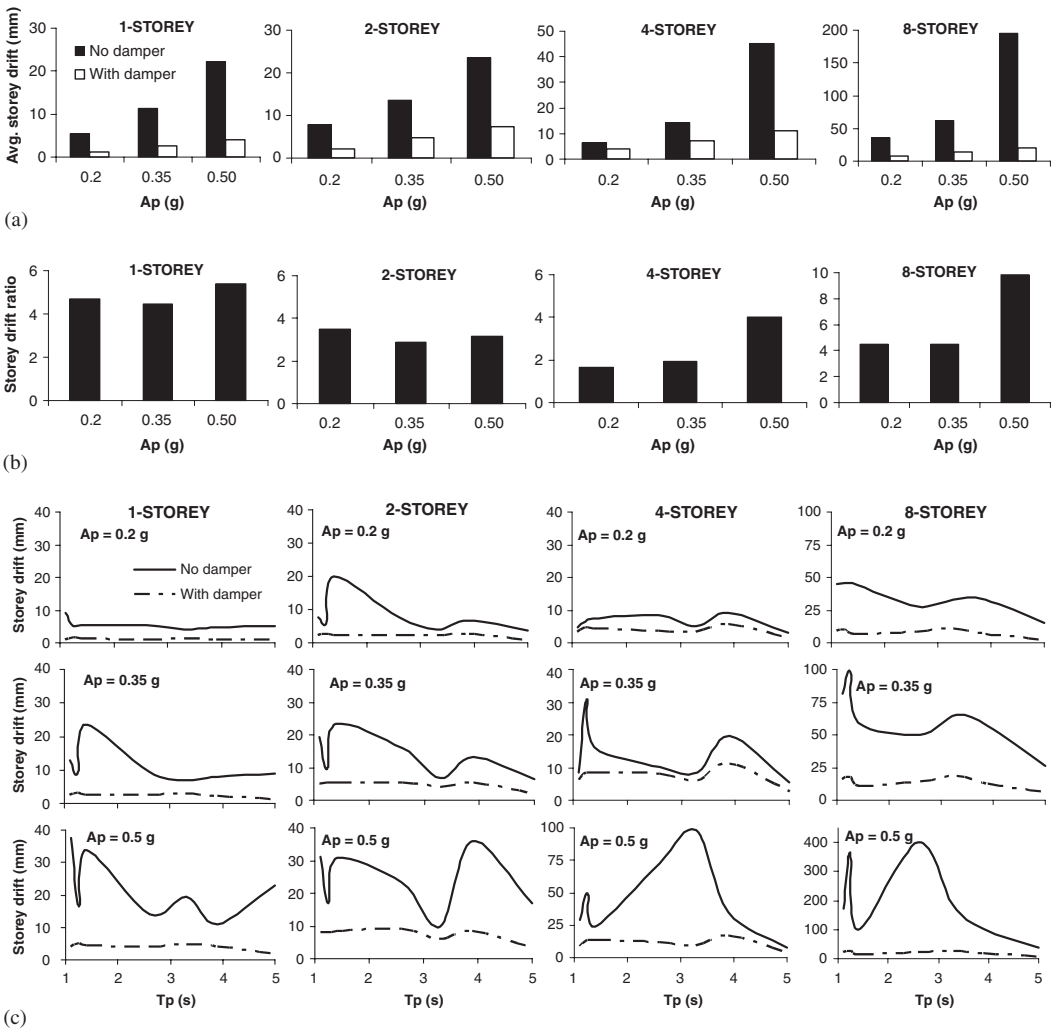

Figure 4. (a) Average of the maximum inter-storey drifts of CBFs with and without FVDs from the seven earthquakes as a function of A_p for one, two, four and eight-storey frames; (b) ratio of the average maximum inter-storey drifts of CBFs without FVDs to those with FVDs for one, two, four and eight-storey frames; and (c) maximum inter-storey drifts of one, two, four and eight-storey CBFs with and without FVDs as a function of T_p for $A_p = 0.20$, 0.35 and $0.50g$.

maximum inter-storey drifts of one, two, four and eight-storey CBFs with and without FVDs as a function of T_p for various ground motion intensities. It is observed that CBFs without FVDs generally display a good response over the range of T_p values considered for low to moderate intensity NF ground motions and for lower number of stories. Nonetheless, for high-intensity NF ground motions and for larger number of stories, a sudden deterioration in the lateral strength and stiffness and an ensuing increase in the maximum drift response of the frames are observed due to the effect of brace buckling and the behaviour of the CBF becomes much more sensitive to the

DOI: 10.1002/eqe

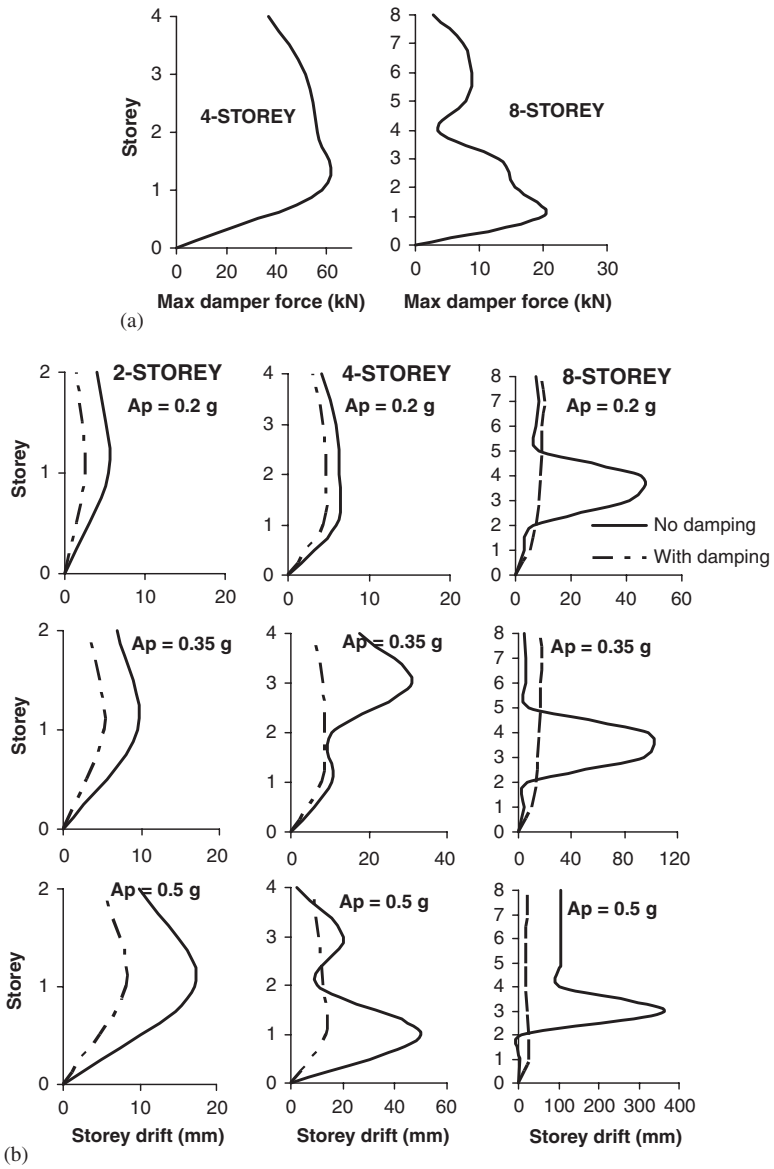

Figure 5. (a) Distribution of damper force along the height of four and eight-storey frames ($A_p = 0.50g$, $T_p = 1.25$ s); and (b) displacement profile of the two, four and eight-storey CBFs with and without FVDs for various A_p ($T_p = 1.25$ s).

T_p of the ground motion. For high-intensity NF ground motions ($A_p = 0.5g$), it is observed from Figure 4(c) that the largest seismic drift responses of the frames with smaller number of stories are generally produced by NF ground motions with lower T_p while those of the frames with larger number of stories are produced by NF ground motions with relatively higher T_p. This may be

DOI: 10.1002/eqe

mainly due to the fundamental inelastic vibration period of the CBFs falling within the range of the dominant period of the NF ground motion. The sensitivity of the response of the CBFs without FVDs to the T_p of the NF ground motion at high intensities makes the performance of such frames unreliable especially in NF regions with high risk of seismic activity.

For CBFs with FVDs, it is observed from Figure 4(c) that the seismic response of the frames is much more uniform than that of the CBFs without FVDs over the range of T_p values considered. Thus, installing FVDs makes the seismic response of the CBF relatively less sensitive to the number of stories and velocity pulse period of the NF ground motion and hence the design and performance of such frames with FVDs become more reliable.

Distribution of FVD forces and effect of FVD on the displacement profile of the CBF

Figure 5(a) presents the distribution of the damper forces along the height of the four and eight-storey frames subjected to a NF ground motion with $A_p = 0.50g$ and $T_p = 1.25$ s. It is observed that generally the damper force decreases at upper storey levels of the frame. This may be mainly due to lower inter-storey displacements (Figure 5(b)) and hence smaller relative damper velocities at higher stories of the frames. Thus, it may be more efficient to place dampers with relatively larger damping capacity at the lower stories of multiple storey CBFs in design or retrofitting applications.

Figure 5(b) compares the deformed shapes of the two, four and eight-storey CBFs with and without FVDs for an NF ground motion with $T_p = 1.25$ s scaled to $A_p = 0.2$, 0.35 and $0.5g$. The deformed shapes of the frames are obtained at the instant when the maximum inter-storey drift occurs. For the CBFs with lower number of stories (up to four stories) and those subjected to lower ground motion intensities ($A_p = 0.2g$), although the FVDs result in much smaller frame lateral displacements, the shape of the displacement profile remains relatively similar to that of the CBFs without FVDs. However for CBFs with higher number of stories subjected to larger ground motion intensities ($A_p = 0.35$ and $0.50g$), the displacement profile of the frames with and without FVDs are totally different. In such frames, the extensive buckling of the braces dominates the behaviour of the CBFs without FVDs where inter-storey drifts much larger than those of the CBFs with FVDs are observed. The buckling of the braces in CBFs without FVDs results in soft-storey formations as observed from Figure 5(b) and concentration of the energy dissipation at the intermediate storey levels. Nevertheless, the CBFs with FVDs exhibit a more uniform lateral displacement profile and distribution of energy demand as well as smaller inter-storey drifts compared to the CBFs without FVDs for all the NF ground motion intensities considered.

Effect of FVD on the hysteretic behaviour and base shear of the CBF

The hysteretic base shear *versus* top displacement behaviours of one and two-storey CBFs without and with FVDs are compared in Figure 6(a) and (b), respectively. For CBFs without FVDs, the adverse effects of brace buckling, which result in stiffness and strength degradation, are clearly observed from the figures. For the CBFs with FVDs, however, the hysteretic performances of the frames become more stable since buckling of the braces is prevented. Furthermore, as observed from the figures, installing FVDs into the CBFs produces larger number of hysteretic cycles. This, in turn, leads to a better energy dissipation mechanism generating smaller frame displacements and base shear forces (i.e. the same earthquake input energy is dissipated by larger number of hysteretic cycles having smaller force and displacement amplitudes).

The effect of FVDs on the maximum base shear force of the one-storey frame is demonstrated in the form of a graph between the maximum base shear force *versus* T_p of the NF ground motions

DOI: 10.1002/eqe

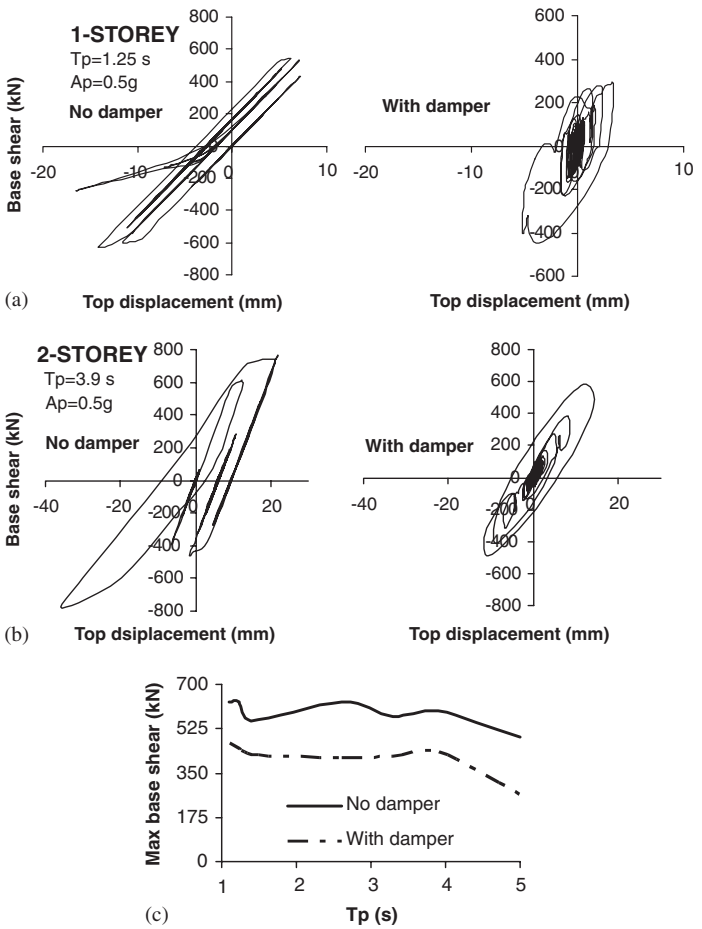

Figure 6. Base shear *versus* top displacement for: (a) one-storey frame; (b) two-storey frame; and (c) comparison of the maximum base shear forces *versus* T_p for one-storey frame.

in Figure 6(c) for $A_p = 0.5g$. It is observed that installing FVDs into CBFs results in a reduction in the base shear force for the range of velocity pulse periods considered. This finding is in agreement with the observations from similar previous research studies on other types of structures [16, 21].

EFFECT OF FVD PARAMETERS ON THE SEISMIC PERFORMANCE OF CBF

In this section, a parametric study involving a total of 224 NLTH analyses is conducted to investigate the effect of FVD parameters on the seismic performance of the frames using one and four-storey CBFs. For this purpose, the damping ratio, ζ, of the frames corresponding to their first vibration mode is varied between 10 and 150% of critical while keeping the value of the velocity exponent, α of the FVDs at 0.5 to solely study the effect of the damping ratio, ζ, on the seismic response of

DOI: 10.1002/eqe

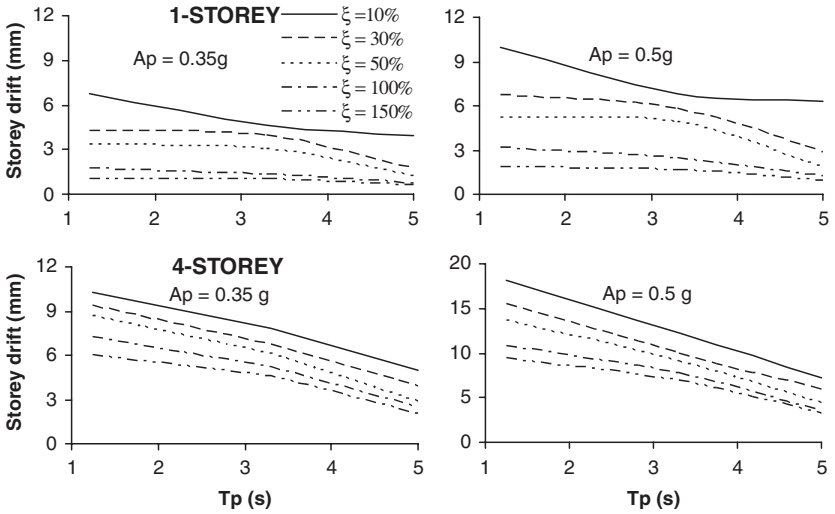

Figure 7. Maximum inter-storey drifts of one and four-storey CBFs with FVDs as a function of T_p for various damping ratios and $A_p = 0.35$ and $0.50g$.

the frames. For each specific ζ value considered, the damping constant C for the FVD is calculated using Equation (2) and assigned to the damper elements in the frame models. Although, values of ζ larger than 50% are not practical, they are considered in the parametric study to measure the benefits of higher percentage of damping on the performance of the frames subjected to NF ground motions. Similarly, keeping the value of the damping ratio, ζ at 50%, the value of the velocity exponent, α, is varied between 0.3 and 1.0 to study the effect of α on the seismic response of the frames. The NLTH analyses results are discussed in the following subsections.

Effect of viscous damping ratio on the seismic performance

Viscous damping ratio versus T_p. Figure 7 displays the maximum inter-storey drifts of the one and four-storey CBFs as a function of the T_p of the ground motions for $\zeta = 10$, 30, 50, 100 and 150% for $A_p = 0.35$ and $0.50g$. It is observed that generally, the maximum inter-storey drift of the CBFs with FVDs decreases as the T_p of the ground motion increases for the range of ζ values and ground motion intensities considered. This is mainly due to the much smaller fundamental periods of the one (0.23 s) and four-storey (0.39 s) frames in relation to the dominant periods of the NF ground motions producing off-resonant, smaller structural responses and hence smaller FVD forces at larger values of T_p. In CBFs without FVDs, however, brace buckling effects and associated lateral stiffness degradation produce inelastic fundamental periods within the range of the period of the NF ground motion leading to large frame responses due to resonance effects. Thus, it becomes clear that one of the main advantages of using FVDs for seismic design and retrofitting of CBFs located in NF zones is to keep the frame within the elastic range and hence produce frame fundamental periods much smaller than the dominant period of the NF ground motions to produce off-resonant, smaller responses.

It is also observed that the variation of the maximum inter-storey drift of the four-storey frame as a function of T_p of the NF ground motion is more precipitous than that of the one-storey frame.

DOI: 10.1002/eqe

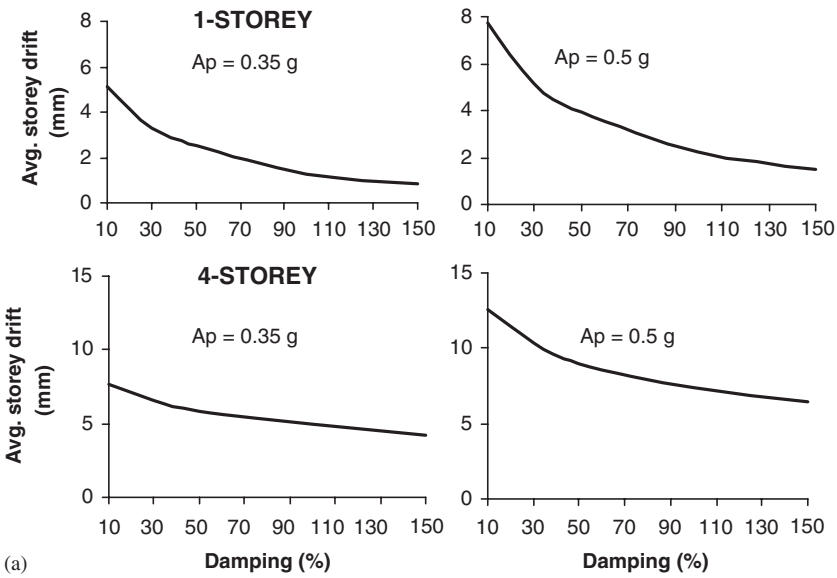

Figure 8. (a) Average of the maximum inter-storey drifts of CBFs with FVDs from the seven earthquakes as a function of the damping ratio for one and four-storey frames and $A_p = 0.35$ and $0.50g$; and (b) maximum damper force as a function of the damping ratio for one-storey frame.

This is mainly associated with the larger fundamental period of the four-storey frame falling within a closer range of the dominant period of the ground motions with lower T_p, thus producing larger inter-storey drifts due to resonance effects. However, for the four-storey frame, the reduction in the maximum inter-storey drifts as a function of the damping ratio seems to be less than that of the one-storey frame. This will be formally investigated in the subsequent section.

Seismic response of the frames versus damping ratio. The average of the maximum inter-storey drifts of the one and four-storey CBFs from the seven NF earthquakes is plotted in Figure 8(a) as a function of the damping ratio for $A_p = 0.35$ and $0.50g$. It is observed that the relationship between the maximum inter-storey drift and the damping ratio is nonlinear and similar regardless of the value of the peak ground acceleration. As expected, the maximum inter-storey drift decreases as

DOI: 10.1002/eqe

the damping ratio increases. However, the reduction in the maximum inter-storey drift as a function of the damping ratio is significant only for damping ratios smaller than or equal to 50%. For ζ values larger than 50%, the relatively smaller reduction in the maximum inter-storey drift of the frame (Figure 8(a)) is accompanied by a relatively large increase in the damper force as observed from Figure 8(b). Thus, in NF zones, using FVDs, which will produce damping ratios larger than 50%, does not seem to be practical. In fact, damping ratios ranging between 10 and 30% seem to produce the largest reduction in the seismic responses while having reasonable damper forces as the curves in Figure 8(a) are steeper within that range. It is also observed that the reduction in the inter-storey drift values becomes totally negligible for damping values larger than critical ($\zeta \geqslant 100\%$). Furthermore, Figure 8(a) reveals that for the four-storey frame, the rate of reduction of the maximum inter-storey drift as a function of the damping ratio is lower than that of the one-storey frame. This is mainly due to the smaller relative damper velocities at higher stories of the four-storey frame (Figure 5(a)) producing less damping effect compared to that of the single-storey frame. Thus, it may be more efficient to place dampers with relatively larger damping capacity at the lower stories of multiple storey CBFs as stated earlier.

Effect of FVD's velocity exponent on the seismic performance

Velocity exponent versus T_p. Figure 9(a) displays the maximum inter-storey drifts of the one and four-storey CBFs as a function of the T_p of the NF ground motions for $\alpha = 0.30$, 0.50, 0.75 and 1.00 for $A_p = 0.35$ and $0.50g$. As observed earlier, the maximum inter-storey drift of the CBFs with FVDs decreases as the T_p of the NF ground motion increases for the range of α values and ground motion intensities considered. It is also observed that the variation of the maximum inter-storey drift as a function of the T_p of the NF ground motions is generally steeper for larger α values. This can be explained as follows.

Assume that the ratio of the damper velocity (V_{D1}) due to an NF ground motion with a lower T_p to that (V_{D2}) due to a NF ground motion with a higher T_p is equal to a constant b. That is, $V_{D1}/V_{D2} = b$ or $V_{D1} = bV_{D2}$. Since for the same peak ground acceleration, NF ground motions with larger T_p produce off-resonant or smaller frame responses as stated earlier, $V_{D1} > V_{D2}$ and, hence the constant, b is larger than 1.0. Accordingly, using Equation (1), the ratio, R_D, of the damper force for a frame subjected to a ground motion with a low T_p to that subjected to a ground motion with a high T_p is expressed as

$$R_D = \frac{CV_{D1}^{\alpha}}{CV_{D2}^{\alpha}} \tag{4}$$

Substituting $V_{D1} = bV_{D2}$, in Equation (4) and simplifying, R_D is expressed as

$$R_D = \frac{C(bV_{D2})^{\alpha}}{CV_{D2}^{\alpha}} = \frac{b^{\alpha}V_{D2}^{\alpha}}{V_{D2}^{\alpha}} = b^{\alpha} \tag{5}$$

The variation of R_D as a function of α is plotted in Figure 9(b) for various damper velocity ratios, b. It is observed from the figure that for smaller α values ($\alpha = 0.3$), the ratio of the damper forces, R_D, for different damper velocity ratios, b, are nearly equal and close to unity. However, for larger α values ($\alpha = 1.0$), the difference between the ratios of damper forces, R_D, for different damper velocity ratios, b, is significant. Consequently, a large difference between the damper forces at low and high T_p values is generally produced for larger α values. This in turn leads to a steeper variation of the maximum inter-storey drift as a function of the T_p of the NF ground motion for

DOI: 10.1002/eqe

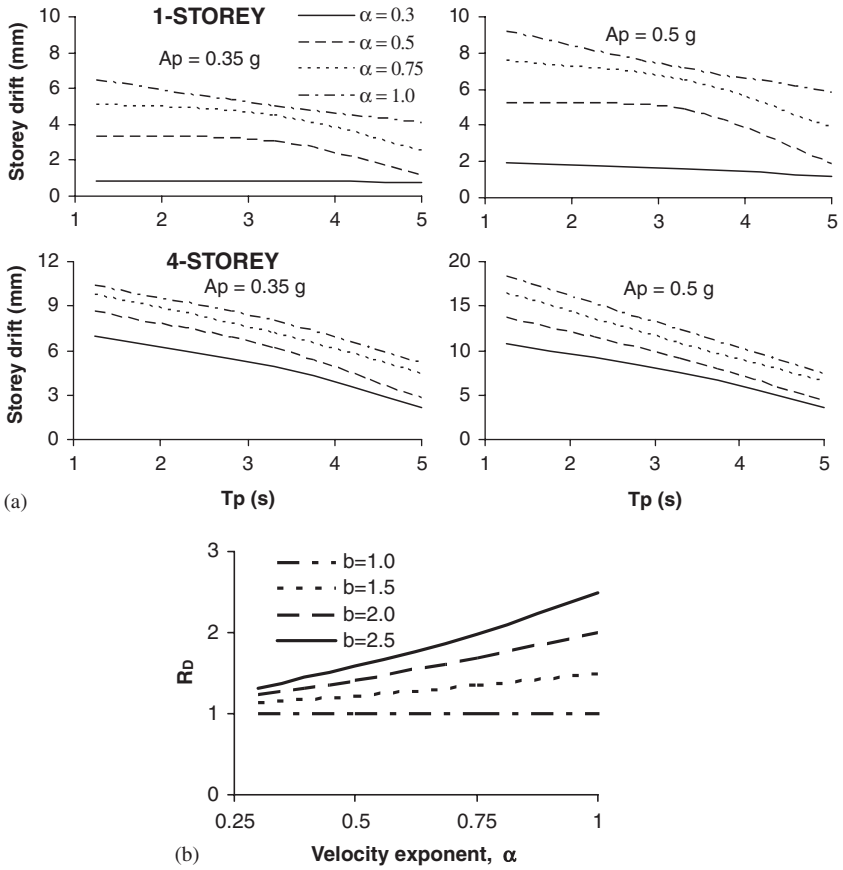

Figure 9. (a) Maximum inter-storey drifts of one and four-storey CBFs with FVDs as a function of T_p for various α values and $A_p = 0.35$ and $0.50g$; and (b) the variation of the damper force ratio, R_D, as a function of the velocity exponent, α, for various damper velocity ratios, b.

larger α values. From the above discussion it may be concluded that using FVDs with smaller α values further reduces the sensitivity of the CBFs to the T_p of the NF ground motion. As a result, the actual performance of the structure becomes more reliable regardless of the velocity pulse period of the NF ground motion used in the design or retrofitting calculations.

The variation of the maximum inter-storey drift of the four-storey frame as a function of the T_p of the NF ground motion is also found to be steeper than that of the one-storey frame for the range of α values considered. As explained earlier, this is mainly associated with the larger fundamental period of the four-storey frame falling within the relatively closer range of the dominant period of the NF ground motions with lower T_p, thus producing larger inter-storey drifts due to resonance effects.

Seismic response of the frames versus velocity exponent. The average of the maximum inter-storey drifts of the one and four-storey CBFs from the seven earthquakes is plotted in Figure 10(a) as a

DOI: 10.1002/eqe

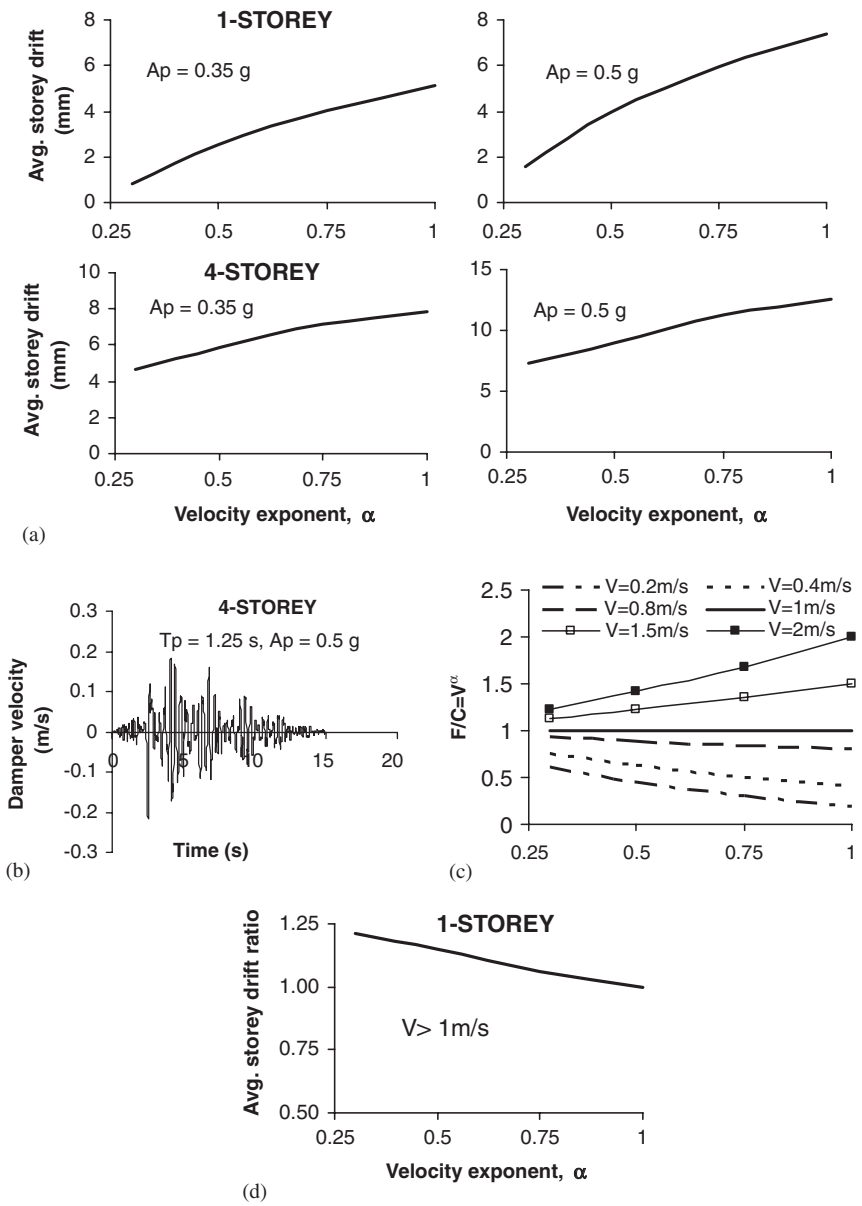

Figure 10. (a) Average of the maximum inter-storey drifts of CBFs with FVDs from the seven earthquakes as a function of the damper velocity exponent for one and four-storey frames and $A_p = 0.35$ and $0.50g$; (b) maximum damper velocity time history for the four-storey frame; (c) variation of normalized damper force with respect to C as a function of velocity exponent for various damper velocities; and (d) average maximum storey drift ratio with respect to the case with $\alpha = 1.0$ from the seven earthquakes as a function of the damper velocity exponent for one-storey frame.

DOI: 10.1002/eqe

function of the velocity exponent, α, for $A_p = 0.35$ and $0.50g$. It is observed that the relationship between the maximum inter-storey drift and the velocity exponent is similar regardless of the value of the peak ground acceleration. The maximum inter-storey drift increases as the velocity exponent increases. This trend results from the values of damper velocities which are smaller than 1.0 m/s for the range of T_p values and ground motion intensities considered in this study as observed from Figure 10(b) where maximum damper velocity within a four-storey frame is plotted as a function of time for an NF ground motion with $A_p = 0.5g$ and $T_p = 1.25$ s. From Equation (1) and Figure 10(c), it is clearly observed that for damper velocities smaller than 1.0 m/s, FVDs with larger α values produce smaller damper resistance, which in turn, leads to larger inter-storey drifts. However, as observed from the same figure (Figure 10(c)), for damper velocities larger than 1.0 m/s, FVDs with larger α values produce larger damper resistance. Consequently, the maximum inter-storey drift decreases as the velocity exponent increases as observed from Figure 10(d) where the average maximum inter-storey drift ratios with respect to the case with $\alpha = 1$ of the one-storey CBF is plotted as a function of the velocity exponent, α, using high ground motion intensities producing damper velocities larger than 1 m/s. Furthermore, Figure 10(a) reveals that for the four-storey frame, the rate of change of the maximum inter-storey drift as a function of the velocity exponent is lower than that of the one-storey frame. This is again mainly due to the smaller relative damper velocities at higher stories of the four-storey frame producing less overall damping effect compared to that of the single-storey frame.

PRACTICAL IMPLICATIONS OF USING FVDs IN NF ZONES

In this section, the practical implications of using FVDs for seismic retrofitting and design of CBFs in NF zones are studied. Figure 11(a) shows the maximum inter-storey drifts of a four-storey CBF without FVDs (zero damping) and with FVDs producing 30 and 50% damping ratio in the first vibration mode. The allowable storey drift limits for building seismic use groups I–III per the International Building Code [34] are also demonstrated on the same plot. The figure is obtained for $\alpha = 0.5$, $T_p = 3.3$ s and $A_p = 0.5g$. As observed from the figure, installing dampers into the

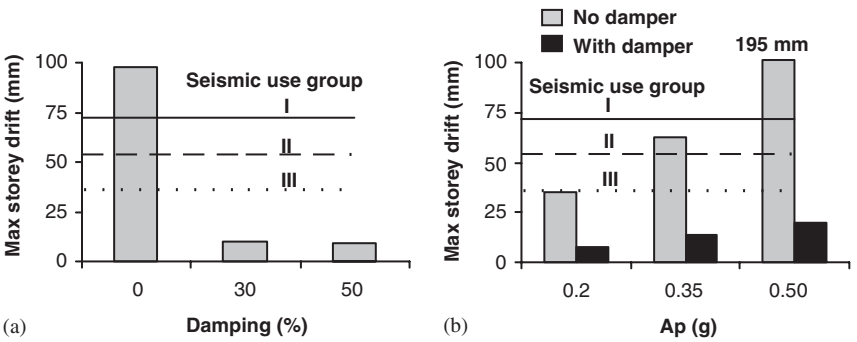

Figure 11. (a) Comparison of code-mandated allowable drifts with those of a four-storey CBF without FVDs and with FVDs having various damping levels ($A_p = 0.50g$, $T_p = 3.3$ s); and (b) comparison of code-mandated allowable drifts with the average of the maximum inter-storey drifts from the seven earthquakes for the eight-storey CBF with and without FVDs for various A_p values.

DOI: 10.1002/eqe

frame system dramatically reduces the large drift values resulting from the buckling of the braces to levels below the code-mandated drift limits. However, larger damping values (e.g. $\zeta = 50\%$) does not seem to benefit the CBFs considerably since a reasonably small value of additional damping (e.g. $\zeta = 10$–30%) is adequate to force the response of the frame into the elastic range (i.e. no brace buckling).

Figure 11(b) displays the average of the maximum inter-storey drifts from the seven NF earthquakes for an eight-storey CBF with and without FVDs for $A_p = 0.20, 0.35$ and $0.50g$. The allowable storey drift limits for seismic use groups I–III per the International Building Code are also demonstrated on the same plot. For the CBFs with FVDs, the figure is obtained for $\zeta = 30\%$ and $\alpha = 0.5$. It is observed from the figure that installing FVDs into the frame system reduces the large drift values resulting from the buckling of the braces to levels below the code-mandated drift limits for the range of A_p values considered. As observed earlier, installing dampers becomes more beneficial for higher ground motion intensities and frames with larger number of stories where brace buckling dominates the behaviour of the CBF (Figures 11(a) and (b)).

In summary, using FVDs with $\zeta = 10$–30% for seismic retrofitting or design of CBFs within the NF zones seems to dramatically improve the response of the frames and produce drift values smaller than those allowed by the building design codes.

CONCLUSIONS AND RECOMMENDATIONS

The effect of FVDs on the seismic performance of CBFs as a function of the intensity and velocity pulse period of the NF ground motion and FVD parameters is investigated. The conclusions are outlined below.

It is observed that CBFs without FVDs generally display a good response over the range of T_p values considered for low to moderate intensity NF ground motions and for lower number of stories. Nonetheless, for high-intensity NF ground motions and for larger number of stories, a sudden deterioration in the lateral strength and stiffness and an ensuing increase in the maximum drift response of the frames are observed due to the effect of brace buckling and the behaviour of the CBF becomes highly sensitive to the T_p of the NF ground motion. The buckling of the braces in CBFs results in soft-storey formations and concentration of the energy dissipation at the intermediate storey levels. Nevertheless, the CBFs with FVDs exhibit a more uniform lateral displacement profile and distribution of energy demand compared to the CBFs without FVDs. Moreover, for CBFs with FVDs, the seismic response of the frames is found to be significantly less sensitive to the T_p of the NF ground motion. Thus, installing FVDs makes the seismic response of the CBF relatively less sensitive to the number of stories and frequency characteristics of the NF ground motion and hence the design and performance of such frames with FVDs become more reliable in NF zones.

Furthermore, it is observed that the presence of FVDs produces significant improvements in the seismic response of the frames in terms of the reduced inter-storey drifts and base shear forces. The energy dissipated by the FVDs prevents the buckling of the braces and causes the frame members to remain within their elastic limits. This, in turn, produces frame fundamental periods much smaller than the dominant period of the NF ground motions leading to off-resonant responses. This results in considerably smaller inter-storey drifts of the CBFs with FVDs than those without FVDs. Furthermore, the calculated inter-storey drifts are found to be less than the code-mandated allowable limits for various building seismic use groups. Moreover, the improvement in the seismic

DOI: 10.1002/eqe

response of the CBFs due to FVDs is found to be more significant than other types of structures such as moment-resisting frames. Thus, using FVDs forms an effective design and retrofit strategy for CBFs and it is generally more useful for frames with larger number of stories located in NF regions with high risk of seismic activity. Furthermore, in retrofitting applications, the presence of the braces in CBFs is anticipated to facilitate the installation of the FVDs at relatively smaller cost compared to other types of structures such as moment-resisting frames.

The parametric studies concerning the effect of damping ratio on the seismic response of the CBFs with FVDs revealed that the relationship between the maximum inter-storey drift and the damping ratio is nonlinear and similar regardless of the value of the peak ground acceleration. As expected, the maximum inter-storey drift decreases as the damping ratio increases. However, the reduction in the maximum inter-storey drift as a function of the damping ratio is significant only for damping ratios smaller than or equal to 50%. For damping ratios larger than 50%, the relatively smaller reduction in the maximum inter-storey drift of the frame is accompanied by a relatively large increase in the damper force. Thus, using FVDs, which will produce damping ratios larger than 50%, does not seem to be practical in NF zones. In fact, damping ratios ranging between 10 and 30% seem to produce the largest reduction in the seismic force while having reasonable damper forces. It is also observed that the reduction in the inter-storey drift values becomes totally negligible for damping values larger than critical ($\zeta \geqslant 100\%$). Furthermore it is found that the relative damper velocities are generally smaller at higher stories producing less damping effect compared to those at lower stories. Thus, it may be more efficient to place dampers with relatively larger damping capacity at the lower stories of multiple storey CBFs.

The parametric studies concerning the effect of the velocity exponent on the seismic response of the CBFs with FVDs revealed that the relationship between the maximum inter-storey drift and the velocity exponent is similar regardless of the value of the peak ground acceleration. For damper velocities smaller than 1 m/s, the maximum inter-storey drift increases as the velocity exponent increases for the range of T_p values and NF ground motion intensities considered in this study. However, for values of damper velocities larger than 1.0 m/s, the maximum inter-storey drift decreases as the velocity exponent increases. Accordingly, using dampers with larger velocity exponent becomes more advantageous in such cases. It is also found that using FVDs with smaller α values further reduces the sensitivity of the CBFs to the T_p of the NF ground motion. As a result, the performance of the structure becomes more reliable regardless of the velocity pulse period of the NF ground motion used in the design or retrofitting calculations.

In summary, it is recommended that using FVDs with damping ratios in the range of 10–30% is very effective for the seismic design and retrofitting of CBFs with large number of stories. Furthermore, for CBFs subjected to intense NF earthquakes, where damper velocities larger than 1 m/s is expected, using FVDs with large α values is very effective for the seismic design and retrofitting of CBFs. However, if the expected damper velocities are smaller than 1 m/s, using FVDs with smaller α values becomes more effective.

REFERENCES

1. Sabelli R, Mahin S, Chang C. Seismic demands on steel braced frame buildings with buckling-restrained braces. *Engineering Structures* 2003; **25**(5):655–666.
2. Khatib IF, Mahin SA, Pister KS. Seismic behavior of concentrically braced steel frames. *Report No. UCB/EERC-88/01*, Earthquake Engineering Research Centre, 1988.
3. Perotti F, Scarlassara GP. Concentrically braced frames under seismic actions: nonlinear behavior and design coefficients. *Earthquake Engineering and Structural Dynamics* 1991; **20**(5):409–427.

DOI: 10.1002/eqe

4. Tremblay R, Robert N. Seismic performance of low- and medium-rise chevron braced steel frames. *Canadian Journal of Civil Engineering* 2001; **28**(4):699–714.
5. Osteraas J, Krawinkler H. The Mexico earthquake of September 19, 1985: behavior of steel buildings. *Earthquake Spectra* 1989; **5**(1):51–88.
6. Kim H, Goel S. Seismic evaluation and upgrading of braced frame structures for potential local failures. *Report No. UMCEE 92-24*, Department of Civil and Environmental Engineering, University of Michigan, Ann Arbor, 1992.
7. Hisatoku TR. Analysis and repair of a high-rise steel building damaged by the 1995 Hyogoken-Nanbu earthquake. *Proceedings of the 64th Annual Convention*, Structural Engineers Association of California, Sacramento, 1995; 21–40.
8. Tremblay R, Timler P, Bruneau M, Filiatrault A. Performance of steel structures during the 1994 Northridge earthquake. *Canadian Journal of Civil Engineering* 1995; **22**(2):338–360.
9. Tremblay R, Bruneau M, Nakashima M, Prion HGL, Filiatrault A, DeVall R. Seismic design of steel buildings: lessons from the 1995 Hyogo-ken Nanbu earthquake. *Canadian Journal of Civil Engineering* 1996; **23**(3):727–756.
10. Krawinkler H, Anderson CJ, Bertero V, Holmes W, Theil C. Northridge earthquake of January 17, 1994: reconnaissance report, vol. 2—steel buildings. *Earthquake Spectra* 1996; **12**(S1):25–47.
11. Malhotra PK. Response of buildings to near-field pulse-like ground motions. *Earthquake Engineering and Structural Dynamics* 1999; **28**(11):1309–1326.
12. Dicleli M, Mehta A. Seismic response of a single storey innovative steel frame system. *Proceedings of the Fifth International Conference on Earthquake Resistant Engineering Structures*, Transactions of the Wessex Institute, Earthquake Resistant Engineering Structures V, Skiathos, Greece, 2005; 259–267.
13. Wilson JC, Wesolowsky MJ. Shape memory alloys for seismic response modification: a state-of-the-art review. *Earthquake Spectra* 2005; **21**(2):569–601.
14. Kamura H, Katayama T, Shimokawa H, Okamoto H. Energy dissipation characteristics of hysteretic dampers with low yield strength steel. *Proceedings of the US–Japan Joint Meeting for Advanced Steel Structures*, Building Research Institute, Tokyo, 2000.
15. Pall AS, Marsh C. Response of friction damped braced frames. *Journal of Structural Engineering* (ASCE) 1982; **108**(ST6):1313–1323.
16. Constantinou MC, Symans MD. Experimental and analytical investigation of seismic response of structures with supplemental fluid viscous dampers. *Report No. NCEER-92-0032*, National Center for Earthquake Engineering Research, State University of New York, Buffalo, NY, 1992.
17. Constantinou MC, Symans MD. Experimental study of seismic response of buildings with supplemental fluid dampers. *Structural Design of Tall Buildings* 1993; **2**(2):93–132.
18. Constantinou MC, Symans MD, Taylor DP. Fluid viscous damper for improving the earthquake resistance of buildings. *Proceedings of the Symposium on Structural Engineering in Natural Hazards Mitigation*, American Society of Civil Engineers, Irvine, California, 1993; 718–723.
19. Martinez-Rodrigo M, Romero ML. An optimum retrofit strategy for moment resisting frames with nonlinear viscous dampers for seismic applications. *Engineering Structures* 2003; **25**(7):913–925.
20. Tsai CS, Ho C-L, Chang C-W, Chen K-C. Experimental investigation on steel structures equipped with fluid viscous damper. *ASME Pressure Vessels and Piping Conference*, American Society of Mechanical Engineers, Pressure Vessels and Piping Division, Seismic Engineering 2001; **428**(2):95–101.
21. Uriz P, Whittaker AS. Retrofit of pre-Northridge steel moment-resisting frames using fluid viscous dampers. *Structural Design of Tall Buildings* 2001; **10**(5):371–390.
22. Clark PW, Kelly JM. Passive control systems for mitigation of near-field earthquake ground motions. *Proceedings of the Conference on Natural Disaster Reduction*, 1996; 217–218.
23. Tirca L-D, Foti D, Diaferio M. Response of middle-rise steel frames with and without passive dampers to near-field ground motions. *Engineering Structures* 2003; **25**(2):169–179.
24. He WL, Agrawal AK. An innovative hybrid control system for civil structures against near-field earthquakes. *Proceedings of the 2004 Structures Congress*, American Society of Civil Engineers, 2004; 769–776.
25. Carden LP, Davidson BJ, Larkin TJ, Buckle IG. Retrofit of seismically isolated structures for near-field ground motion using additional viscous damping. *Bulletin of the New Zealand Society for Earthquake Engineering* 2005; **38**(2):106–118.
26. ADINA. *Automatic Dynamic Incremental Nonlinear Analysis*, *Version 8.2*. ADINA R&D, Inc., Watertown, MA, 2004.
27. Makris N, Black CJ. Evaluation of peak ground velocity as a 'good' intensity measure for near-source ground motions. *Journal of Engineering Mechanics* (ASCE) 2004; **130**(9):1032–1044.

DOI: 10.1002/eqe

28. Soong TT, Spencer Jr BF. Supplemental energy dissipation: state-of-the-art and state-of-the-practice. *Engineering Structures* 2002; **24**(3):243–259.
29. BSSC. *NEHRP Recommended Provisions for the Development of Seismic Regulations for New Buildings and Other Structures*. Federal Emergency Management Agency, Washington, DC, 1997.
30. Tedesco JW, McDougal WG, Ross CA. *Structural Dynamics Theory and Applications*. Addison-Wesley: Menlo Park, 1999.
31. Black GR, Wenger BA, Popov EP. Inelastic buckling of steel struts under cyclic load reversals. *Report No. UCB/EERC-80/40*, Earthquake Engineering Research Centre, 1980.
32. Bruneau M, Uang CM, Whittaker A. *Ductile Design of Steel Structures*. McGraw-Hill: New York, 1998.
33. Dicleli M, Mehta A. Simulation of inelastic cyclic buckling behavior of steel box sections. *Computers and Structures* 2007, in-print.
34. ICC. *International Building Code*. International Code Council, Falls Church, Virginia, 2000.

DOI: 10.1002/eqe